Bunch Compression in the International Linear Collider

Kellen Petersen
Department of Physics, University of Utah, Salt Lake City, Utah, 84112
(Dated: August 12, 2005)

Damping rings in linear colliders produce bunches much longer than required by the main linac. Therefore, an intermediate process is required to produce bunches with the desired length. Bunch compressors fulfill this requirement by reducing the bunch length through rotations of the longitudinal phase space while increasing the rms energy spread. There are many possible ways of accomplishing this task and it is the purpose of this paper to compare various bunch compressor designs and to present studies of some current designs for the International Linear Collider.

I. INTRODUCTION

To achieve high peak luminosity [1] at the interaction point, the bunches in the main linac of the International Linear Collider (ILC) need to have rms lengths between 100 and 500 μm. However, the ILC damping rings produce bunches about 6 mm long which are much larger than the set parameter (and it has been proposed that the rms bunch length from the damping rings be increased since damping rings are made easier with longer bunches [2]). Consequently, it is necessary to compress the bunch before injection into the main linac [3]. In this paper, different proposed designs will be described beginning with a single-stage bunch compressor. We shall also compare two current two-stage bunch compressor configurations. Design studies include calculation of Twiss parameters and simulations of longitudinal phase space distributions, emittance preservation, orbit with a one σ_y (where σ_y is the vertical beam size) vertical offset, emittance growth due to incoherent synchrotron radiation, and longitudinal tolerances.

II. BUNCH COMPRESSOR DESIGNS

There exist various bunch compressor configurations designed to achieve the required ILC parameters. Some proposed configurations include a single-stage compression design, four two-stage compression designs and a three-stage compression design. The single-stage design compresses the rms bunch length from 6 mm to 300 μm using an initial RF section and a wiggler based on the Tesla TDR design [4].

We began the studies reported here by looking at the Generation One (G1)[1] single-stage bunch compressor. Our results were compared to earlier SLAC results on the same design. This was done in part to verify the results obtained at SLAC based on simulations using Lucretia [5] and also to study bunch compression lattices with TAO [6] while checking its simulation performance. A single-stage bunch compressor is advantageous because it achieves an rms bunch length of 300 μm at a reduced cost since a single-stage design is shorter in length than multi-stage bunch compressors. However, there are a few drawbacks to the

[1] G1 stands for Generation 1 (the first bunch compressor designs for the ILC) and subsequent designs are labelled G2, G3, ...

single-stage design, which include: the final rms relative energy spread is large (greater than 3%), the design cannot achieve a 150 μm rms bunch length without producing an impractically large rms energy spread, and strong nonlinear effects necessitate overcompression of the bunch resulting in an even larger energy spread allowing for potentially large emittance growth.

Following the studies of the G1 single-stage compression design, Generation 3 two-stage designs were studied. There exist four different configurations for the two-stage design (150A, 150B, 300A, and 300B); however, only results of studies on the first two are reported here. The number in the design name represents the desired final rms bunch length leaving the bunch compressor and the letter indicates the manner in which the longitudinal phase space rotation occurs. Variant "A" involves two 90° rotations of the longitudinal phase space with one rotation occuring in each stage of the bunch compressor. Variant "B" results in a total rotation of only 90°, and is sometimes referred to as a design involving an "undercompression" [7] in its first stage.

III. STUDIES OF THE G1 SINGLE-STAGE BUNCH COMPRESSOR

In studying the single-stage design, the injected beam had an initial energy of 5 GeV with an rms energy spread of 0.15% and an initial rms bunch length of 6 mm. The parameters of this configuration are listed in Table I and it is noted that it was designed to compress the rms bunch length to 300 μm; however, to achieve this compression the rms energy spread is increased to 4.13% with a final energy of 4.37 GeV.

TABLE I: Beam parameters for the G1 single-stage bunch compressor

Parameter	G1 Single Stage
Initial Energy [GeV]	5.0
Initial RMS Energy Spread [%]	0.15
Initial RMS Bunch Length [mm]	6.0
BC Voltage [MV]	1275
BC Phase [deg]	-119.5
BC R_{56} [mm]	-147.5
End BC Energy [GeV]	4.37
End RMS BC Energy Spread [%]	4.13
End RMS BC Bunch Length [mm]	0.3

A. Twiss Parameters

Figure 1 shows the beta functions for the bunch compressor and for the full system from the entrance of the bunch compressor to exit of the main linac. These plots are consistent with those obtained using Lucretia at SLAC [8]. Below, A and B are the normal-mode plots of the Twiss parameters.

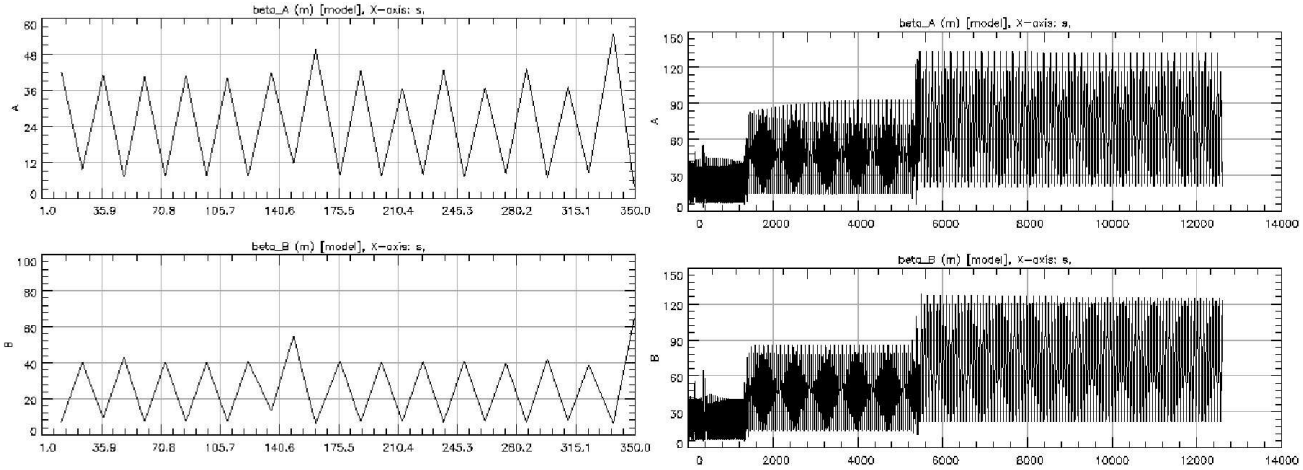

FIG. 1: Beta function for the bunch compressor (left) and the full system (right) for the G1 single-stage design

B. Phase Space Distribution

The following plots show the longitudinal phase space distribution of the particles for each stage of the system. The nonlinear effects of the bunch compressor are apparent in the phase space plots, indicated by the asymmetry that appears after the bunch compressor and after the linac. Also, the centroid energy of the bunch after the linac has been reduced by the wakefields.

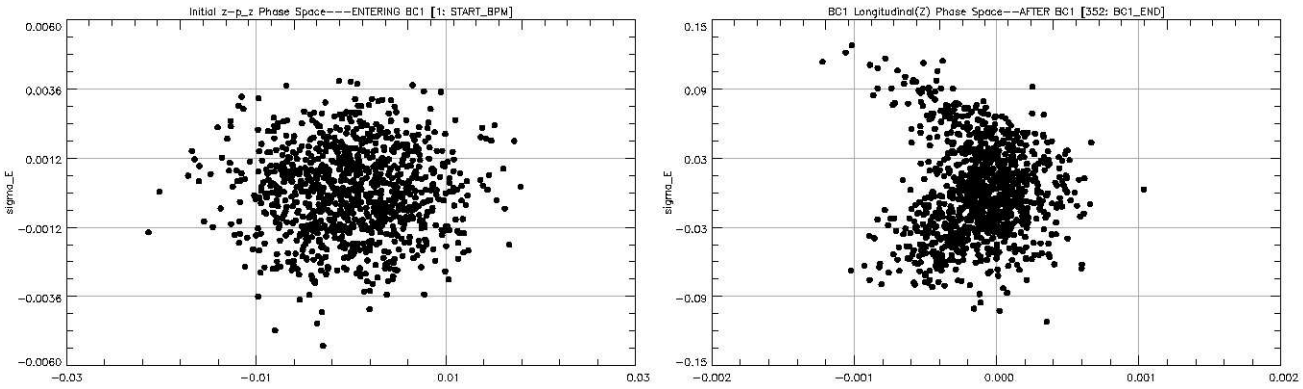

FIG. 2: Phase space distribution plots for the G1 single-stage design: initial (left) and after the bunch compressor (right)

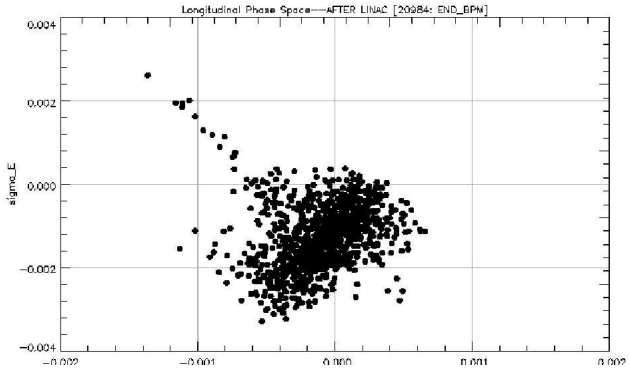

FIG. 3: Phase space distribution plot for the G1 single-stage design: end of the main linac

C. Emittance Preservation

In the studies done concerning emittance preservation in a perfectly aligned machine, the emittance growth was studied for a beam entering the bunch compressor on-axis and then with a one σ_y vertical offset, where σ_y is the vertical beam size. For a beam entering on-axis the horizontal emittance growth is about 1% with a vertical emittance growth of 5%. However, if the beam enters off-axis by one σ_y then the vertical emittance growth increases to 55%, as expected for this situation.

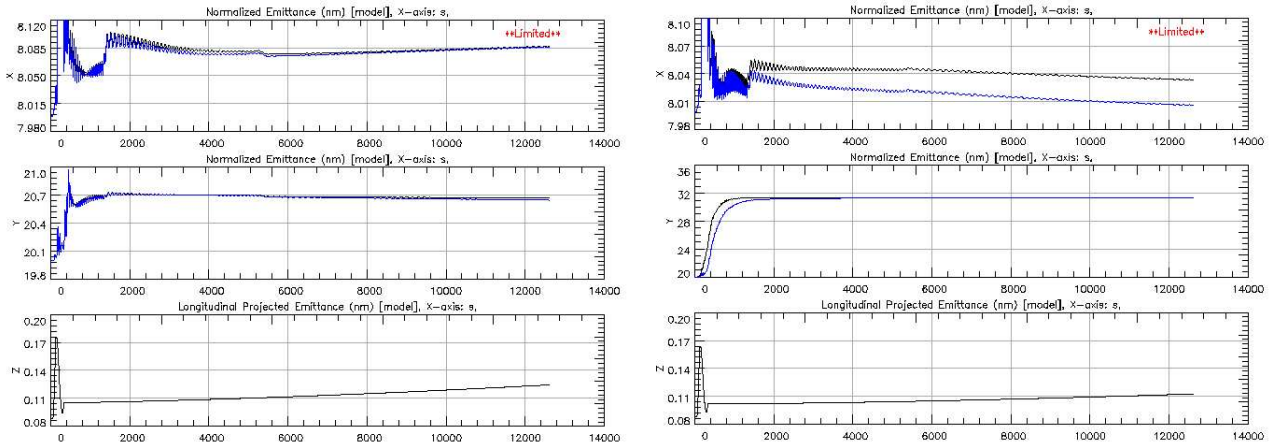

FIG. 4: Comparison of normalized emittance for G1 single-stage design with on-axis beam (left) and one σ_y vertical offset (right): projected (black) and normal-mode (blue)

D. Orbit

The orbit for this design was also studied when a beam enters off-axis by a one σ_y vertical offset. The figures below are the plots of the absolute vertical orbit and the vertical orbit normalized to σ_y. From these simulations it appears that the amplitude of the vertical orbit decreases rapidly while in the bunch compressor and approaches zero while in the main linac. However, the normalized vertical orbit appears to approach zero in the early portion of the linac and then grows slightly as it approaches the end of the linac.

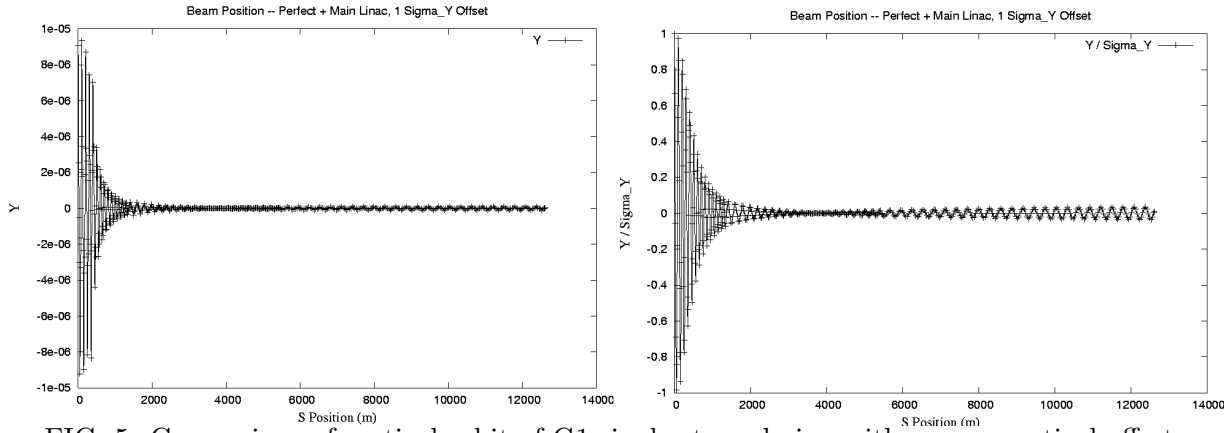

FIG. 5: Comparison of vertical orbit of G1 single-stage design with one σ_y vertical offset: absolute (left) and normalized (right)

E. Longitudinal Tolerances

The manner in which bunch compression operates is through a rotation of the longitudinal phase space of the bunch. The tolerance and sensitivity to a range of errors are a concern and are addressed here. We present results indicating how sensitive energy, energy spread, arrival time, and bunch length are to damping ring extraction errors and to RF phase and amplitude errors. In the following sensitivity plots, the G1 single-stage results from TAO are compared with those from Merlin [9]. Of special concern is the arrival time error since the beams must collide at the focal point of the interaction region to achieve maximum luminosity [10]. Since arrival time is important, note the good agreement between the two codes which both show a small arrival time sensitivity to damping ring extraction phase variations. However, the arrival time shows sensitivity to both RF phase and amplitude variations.

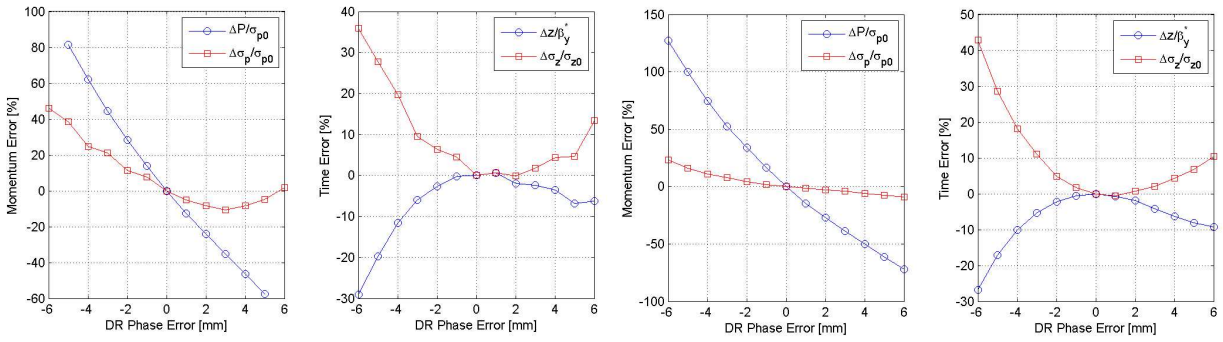

FIG. 6: Damping ring (DR) phase extraction error comparison of G1 single-stage design: TAO (left) vs. Merlin (right)

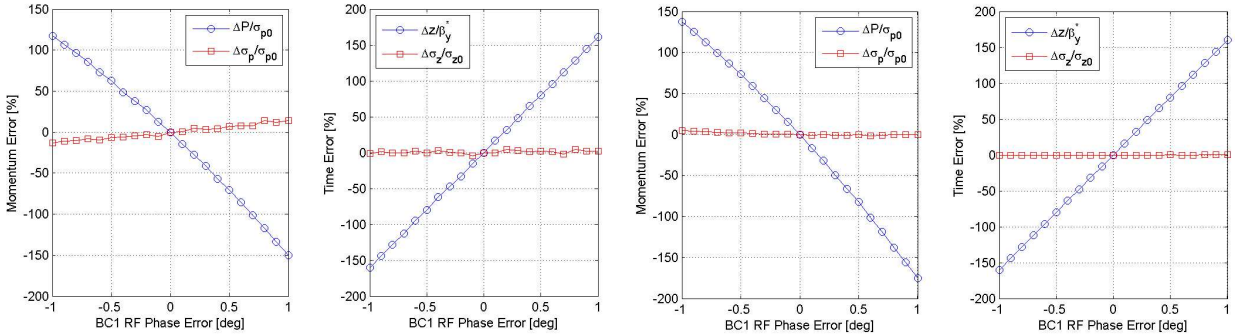

FIG. 7: Bunch compressor RF phase error comparison of G1 single-stage design: TAO (left) vs. Merlin (right)

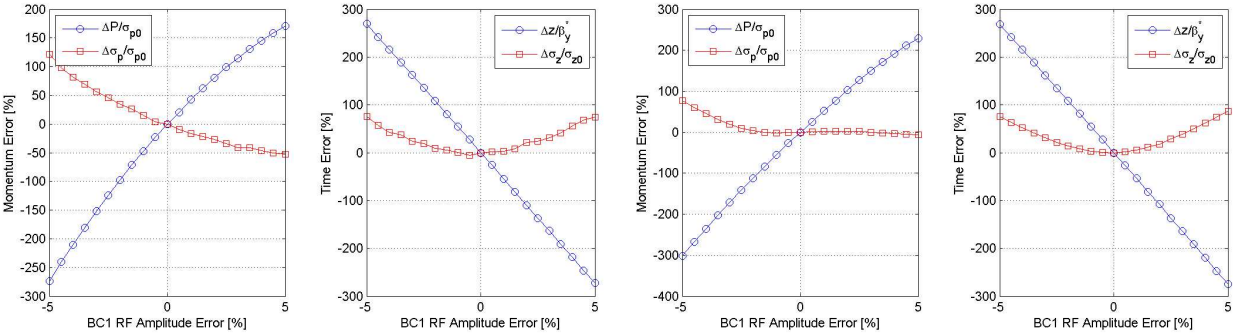

FIG. 8: Bunch compressor RF amplitude error comparison of G1 single-stage design: TAO (left) vs. Merlin (right)

IV. STUDIES OF THE G3 TWO-STAGE 150A AND 150B BUNCH COMPRESSORS

Based on the first and second generations of bunch compressors, a Generation 3 (G3) bunch compressor design was developed. The G1 two-stage designs achieve bunch compression in two stages with acceleration of the bunch in between. This design was developed to keep the rms energy spread small since it is that which produces disperive emittance growth in the main linac. Compared to the G1 design, the G3 design includes larger quadrupole magnet spacing and smaller FODO cell phase advance which was configured to reduce dispersive emittance growth. The new G3 designs also allow adjustment of the momentum compaction without having to realign the quadrupole magnets [11]. This flexibility results in a design that allows multiple configurations to be represented as a single lattice with different configurations achieved simply by adjusting magnet strengths and RF amplitudes and phases. The following presents a comparison of the two configurations which are designed to shorten the rms bunch length from 6 mm to 150 μm.

The initial beam properties are the same for all studies done on the bunch compressor designs and are listed in Table II.

As mentioned above, the G3 designs are based on the G1 designs however some changes were made. Therefore it is useful to compare the properties of the bunch compressors and the differences between the two designs (Table III). The newer G3 design has lower voltages

TABLE II: Beam properties at injection into bunch compressors

Property	Value
Charge	2×10^{10} (3.2 nC)
Energy	5 GeV
RMS Energy Spread	0.15%
RMS Bunch Length	6 mm

in each in stage of the compression than the G1 design while the phases are the same in the first stage and larger in the second. Also, of importance, are the differences between the R_{56} coefficient of each stage.

TABLE III: Comparison of first and third generations 150A and 150B bunch compressor design parameters

Parameter	G1 150A	G3 150A	G1 150B	G3 150B
BC1 Voltage [MV]	270	253	610	580
BC1 Phase [deg]	-100	-100	-110	-110
BC1 R_{56} [mm]	-700	-750	-260	-267
BC2 Voltage [MV]	15000	12750	13000	11600
BC2 Phase [deg]	-48	-58	-38	-45
BC2 R_{56} [mm]	-52	-41	-52	42

In Table IV the energy, rms energy spread, and rms bunch length after each stage of the compression are compared between the first and third generations' configurations for the 150A and 150B designs. From the studies done on the G3 150A and G3 150B designs, we see that after the first stage of compression the energies are near the energies of the earlier G1 designs; however, the rms energy spread is less and rms bunch lengths are larger. Then, after the second stage of compression the final rms bunch lengths are the same but the G3 designs have a lower total energy resulting in a larger relative rms energy spread (Table IV).

TABLE IV: Energy, rms energy spread, and rms bunch length of the 150A and 150B designs of the first and third generations of bunch compressors

	G1 150A	G3 150A	G1 150B	G3 150B
Initial Energy [GeV]	5.0	5.0	5.0	5.0
Initial RMS Energy Spread [%]	0.15	0.15	0.15	0.15
Initial RMS Bunch Length [mm]	6.0	6.0	6.0	6.0
End BC1 Energy [GeV]	4.95	4.96	4.79	4.80
End BC1 RMS Energy Spread [%]	0.90	0.82	1.96	1.83
End BC1 RMS Bunch Length [mm]	1.06	1.14	1.00	1.12
End BC2 Energy [GeV]	15.0	11.7	14.9	13.0
End BC2 RMS Energy Spread [%]	2.03	2.73	1.96	2.46
End BC2 RMS Bunch Length [mm]	0.15	0.15	0.15	0.15

A. Twiss Parameters

In the Twiss parameter studies for the G3 150A and G3 150B designs, the beta functions were plotted for the individual bunch compressor configurations. The left figures are the beta functions through the bunch compressor and the right figures are the beta functions for the full system (bunch compressor and main linac). The areas where the beta functions are largest are areas of acceleration through RF cavivities. The results from the studies using TAO are consistent with those of Lucretia [11].

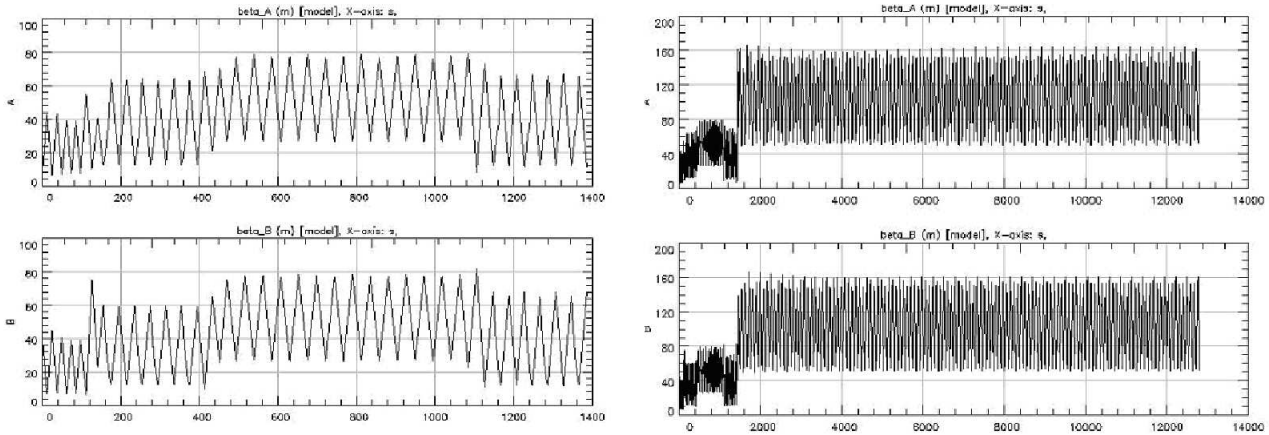

FIG. 9: Beta function for the G3 150A bunch compressor (left) and the full system (right)

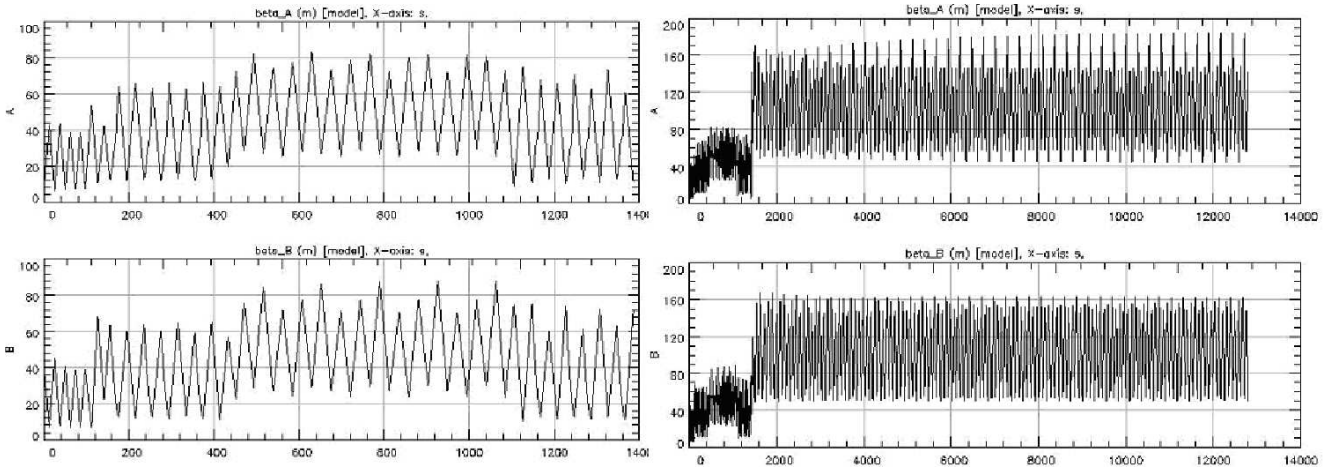

FIG. 10: Beta function for the G3 150B bunch compressor (left) and the full system(right)

B. Phase Space Distribution

As with the G1 single-stage design, there is initially a guassian distribution of particles that enter the bunch compressor. After the first stage in both the G3 150A and G3 150B designs, the rms bunch lengths are shortened to about 1 mm and the rms energy spreads increase to 0.82% (150A) and 1.83% (150B) with the nonlinear effects almost unnoticable. Then, after the second stage, the rms bunch lengths are shortened to the desired 150 μm and again the rms energy spreads increase, but with a more noticable effect of the nonlinearities

involved. As pointed out early, the rms energy spread of the newer G3 designs are larger than their related G1 designs since the total final energy is less. In comparison to the single-stage design, the rms bunch lengths are half as long, the rms relative energy spreads at comparable energies are lower, and the phase space distributions after the bunch compressor are more symmetric.

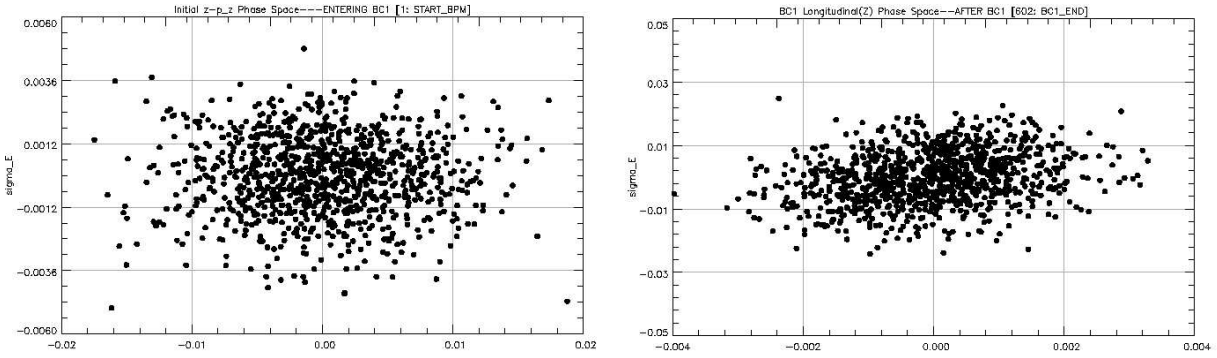

FIG. 11: Phase space distribution plots for the G3 two-stage 150A design: initial (left) and after the BC1 (right)

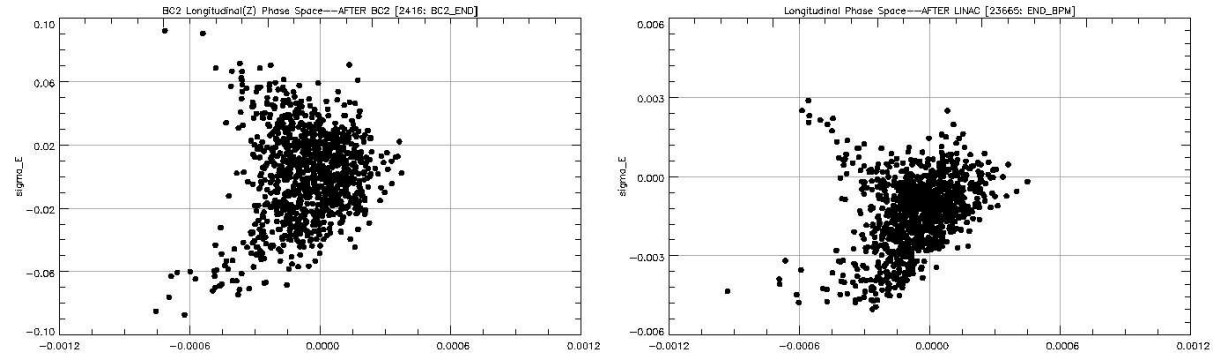

FIG. 12: Phase space distribution plots for the G3 two-stage 150A design: after BC2 (left) and at end of main linac (right)

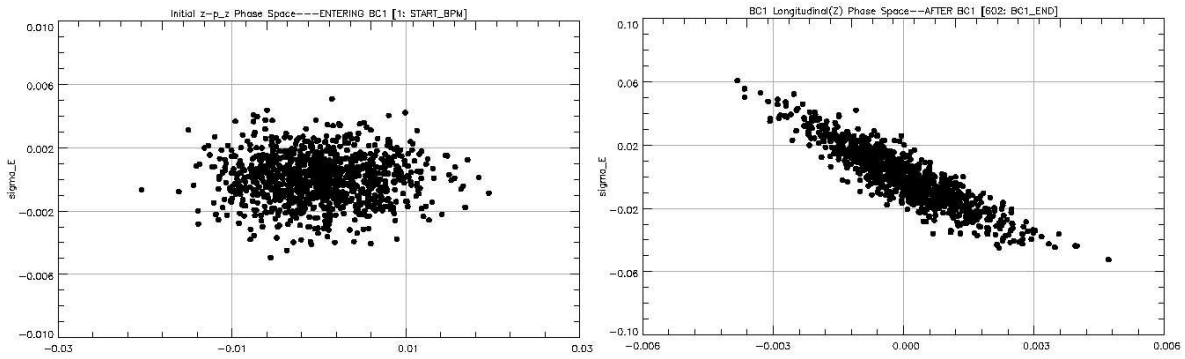

FIG. 13: Phase space distribution plots for the G3 two-stage 150B design: initial (left) and after the BC1 (right)

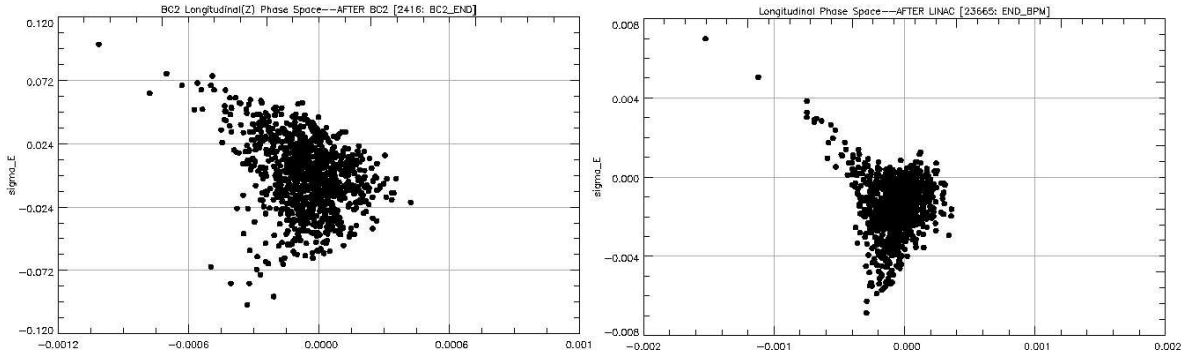

FIG. 14: Phase space distribution plots for the G3 two-stage 150B design: after BC2 (left) and at end of main linac (right)

C. Emittance Preservation

In analyzing the emittance preservation for these two designs, the same studies were done as with the G1 single-stage design. With a perfectly aligned machine, the emittance growths of on-axis and vertically offset beams are compared. For both the G3 150A and G3 150B designs the emittances are nearly preserved for beams entering on-axis. However, for beams vertically offset one σ_y the vertical emittance growths are 25% and 40%, respectively.

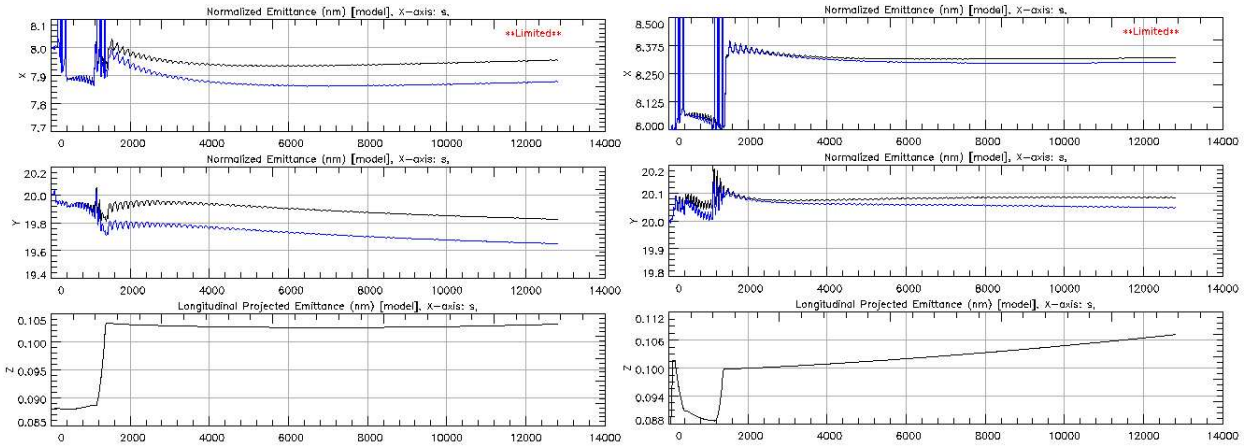

FIG. 15: Normalized emittance comparison of G3 150A (left) and G3 150B (right) with on-axis beam: projected (black) and normal-mode (blue)

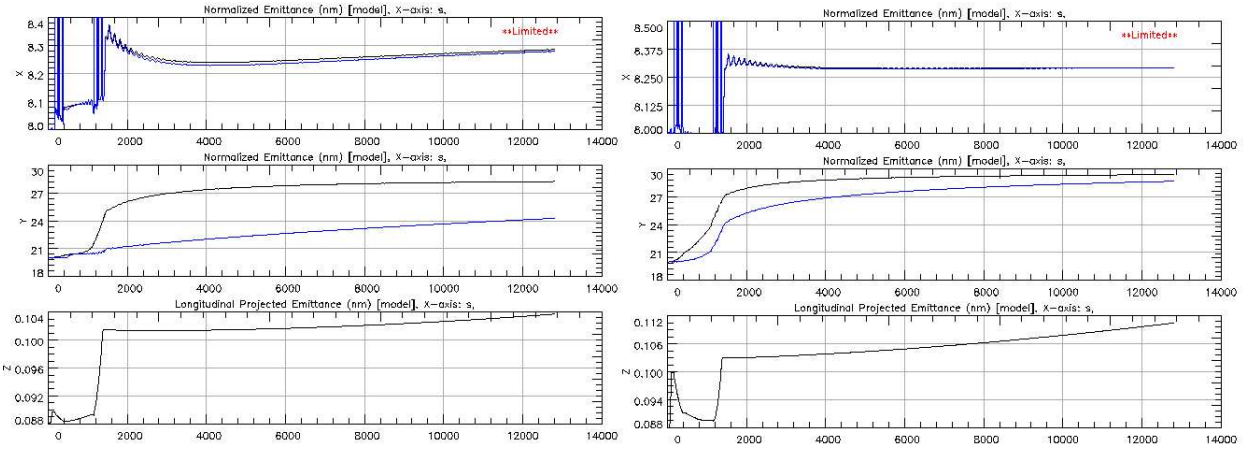

FIG. 16: Normalized emittance comparison of G3 150A (left) and G3 150B (right) with one σ_y vertical offset: projected (black) and normal-mode (blue)

D. Orbit

To study the orbits of these designs, a one σ_y vertically offset beam is considered. The vertical orbit in the G3 150A design decreases to half of the initial orbit while in the bunch compressor and decreases more while in the main linac, but with an orbit amplitude of 1-2 μm. In comparison, the G3 150B design decreases more in the main linac than the latter. In contrast to the single-stage design, these two designs have a somewhat large normalized vertical orbit in the main linac, with the G3 150A design's normalized orbit decreasing to only 0.5.

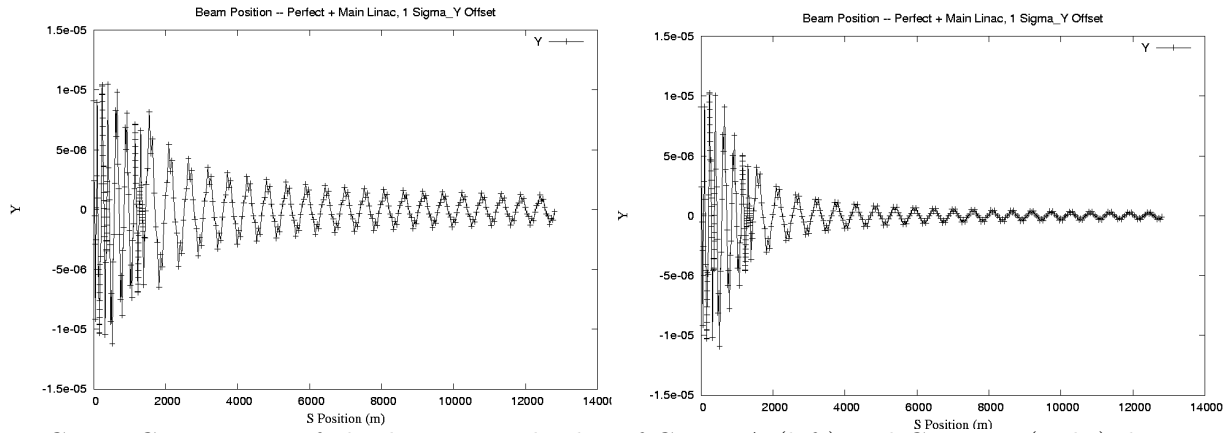

FIG. 17: Comparison of absolute vertical orbit of G3 150A (left) and G3 150B (right) designs with one σ_y vertical offset

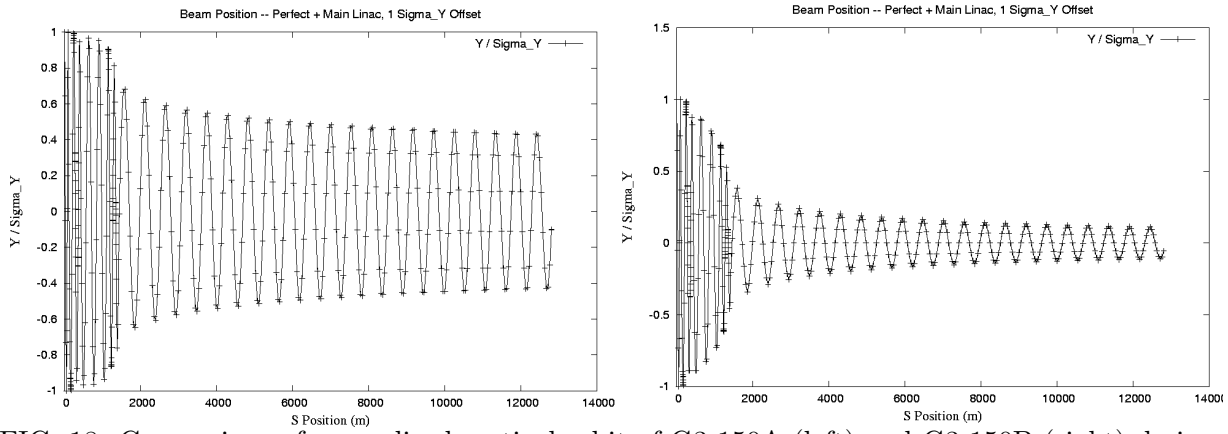

FIG. 18: Comparison of normalized vertical orbit of G3 150A (left) and G3 150B (right) designs with one σ_y vertical offset

E. Emittance Growth from Incoherent Synchrotron Radiation

When relativistic particles pass through a magnetic field they are forced to travel a circular path and synchrotron radiation is emitted. Therefore, synchrotron radiation is produced in the wigglers of the bunch compressor and is a potential cause of emittance growth. Present parameters for the luminosity of the International Linear Collider allow only 20-25% emittance growth in the whole system and it is desired that the synchrotron radiation emittance growth in the bunch compressor remains below 4% [12].

The horizontal emittance growth from synchrotron radiation has been calculated for each of the G3 two-stage bunch compressor configurations. These calculations were done both analytically and through simulations using the program TAO.

The analytical form of the emittance growth from incoherent synchrotron radiation is given by [13]:

$$\Delta(\gamma\epsilon) = \frac{2}{3} C_q r_e \gamma^6 I_5 \tag{1}$$

where C_q is a quantum constant, r_e is the classical radius of the electron and I_5, is the fifth synchrotron integral [14]. Therefore, the emittance growth is proportional to the sixth power of the energy and to I_5, which has a value depending on the parameters and design of the bunch compressor. That is,

$$I_5 = \sum_{dipoles} \int \frac{H}{|\rho|^3} ds \tag{2}$$

with the H-function, $H = \gamma\eta^2 + 2\alpha\eta\eta' + \beta\eta'^2$, being expressed in terms of the dispersion and the Twiss parameters.

In the calculations using TAO simulations, 100,000 particles were tracked, for twelve seeds, through each bunch compressor configuration with radiation turned on. Then, the horizontal emittance growth was calculated using values for the normalized, normal-mode emittance. There was good agreement between the two methods. Table V contains a comparison of the calculated values of the emittance growth from incoherenct synchrotron radiation for all four G3 two-stage bunch compressor designs. It is important to note that variant "A" bunch compressor designs produce larger emittance growth from synchrotron radiation than variant "B", because of its much larger R_{56} coefficient in the first stage of compression [15].

TABLE V: Comparison of synchrotron radiation emittance growth for G3 bunch compressors

	G3 150A	G3 150B	G3 300A	G3 300B
Analytic	2.49%	0.73%	3.57%	2.70%
Tracking	2.74%	0.83%	3.65%	2.74%

F. Longitudinal Tolerances

The same longitudinal sensitivity studies were done for the G3 150A and G3 150B designs as were done for the G1 single-stage design. The following plots of the sensitivity studies for the G3 designs were calculated from data using TAO and are compared with the sensitivity studies of the similar G1 designs calculated from Merlin. As mentioned in the G1 single-stage design study, the correct arrival time is important to create high luminosity. As is apparent in the following plots, the newer G3 designs show improvement in less arrival time sensitivity to damping ring (DR) extraction errors compared to the G1 designs. The G3 150A design also shows less sensitivity to BC1 RF phase and amplitude errors than the G1 150A design.

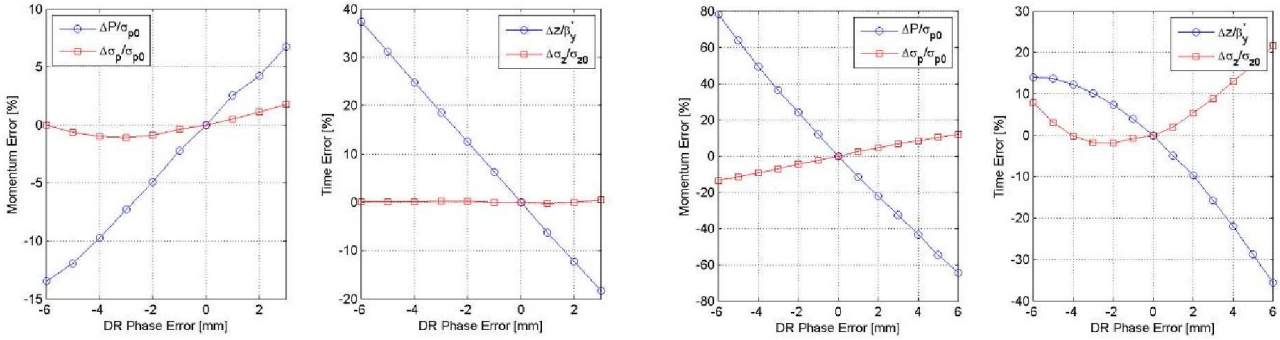

FIG. 19: DR extraction phase error comparison (Merlin): G1 150A (left) vs. G1 150B (right)

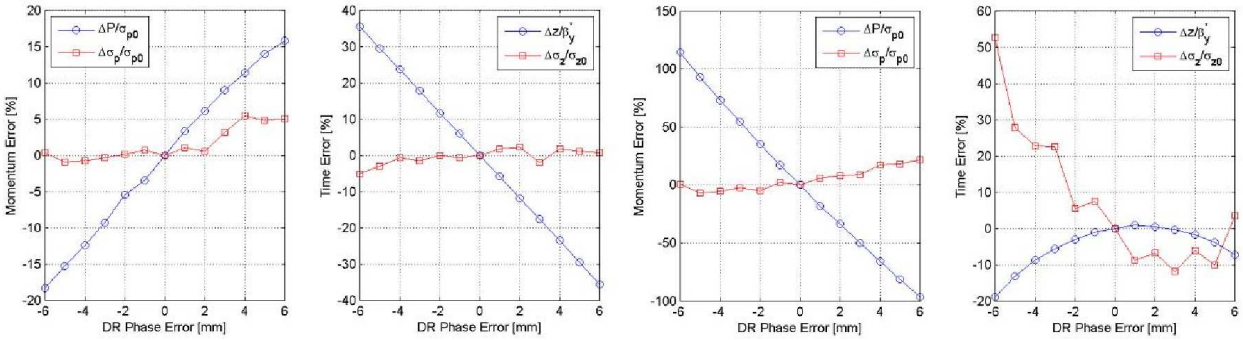

FIG. 20: DR extraction phase error comparison (TAO): G3 150A (left) vs. G3 150B (right)

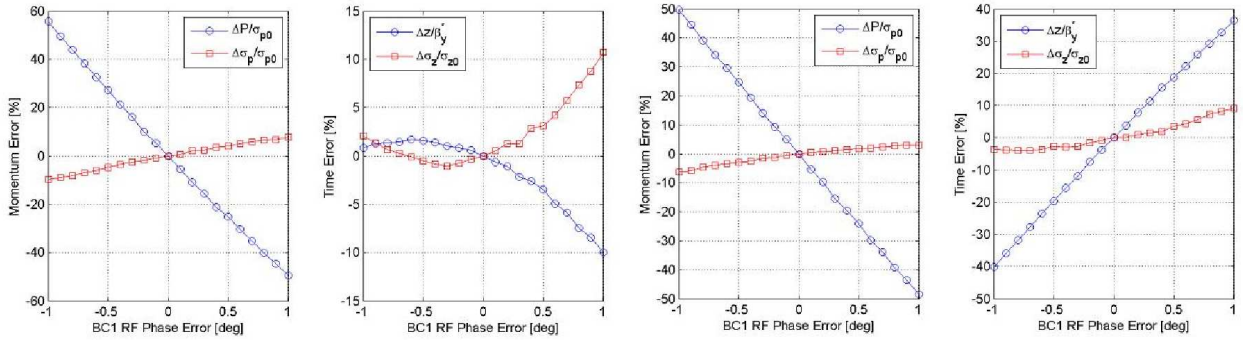

FIG. 21: BC1 RF phase error comparison (Merlin): G1 150A (left) vs. G1 150B (right)

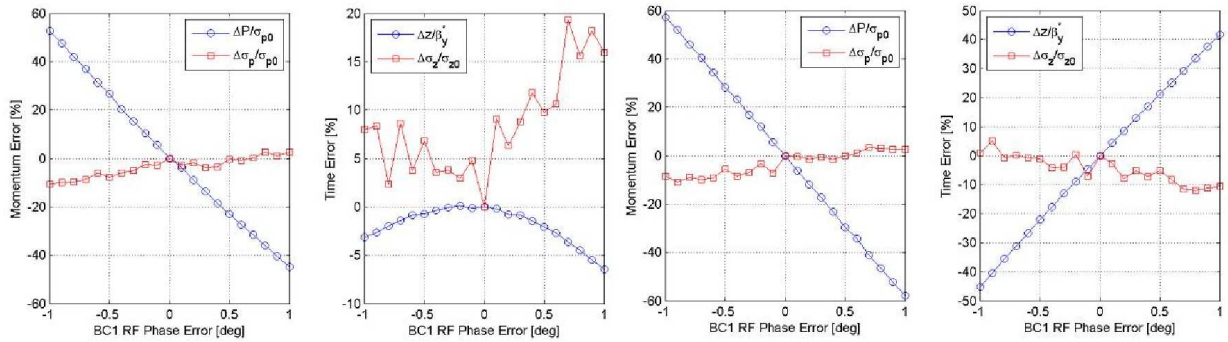

FIG. 22: BC1 RF phase error comparison (TAO): G3 150A (left) vs. G3 150B (right)

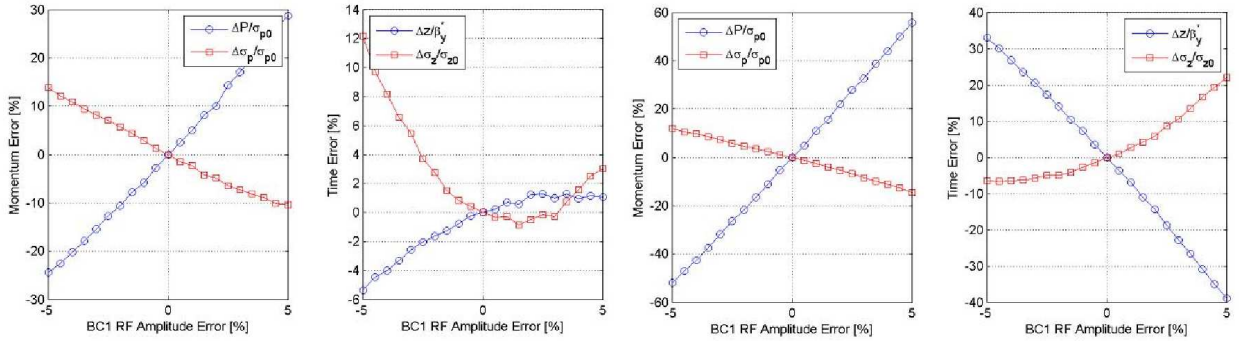

FIG. 23: BC1 RF amplitude error comparison (Merlin): G1 150A (left) vs. G1 150B (right)

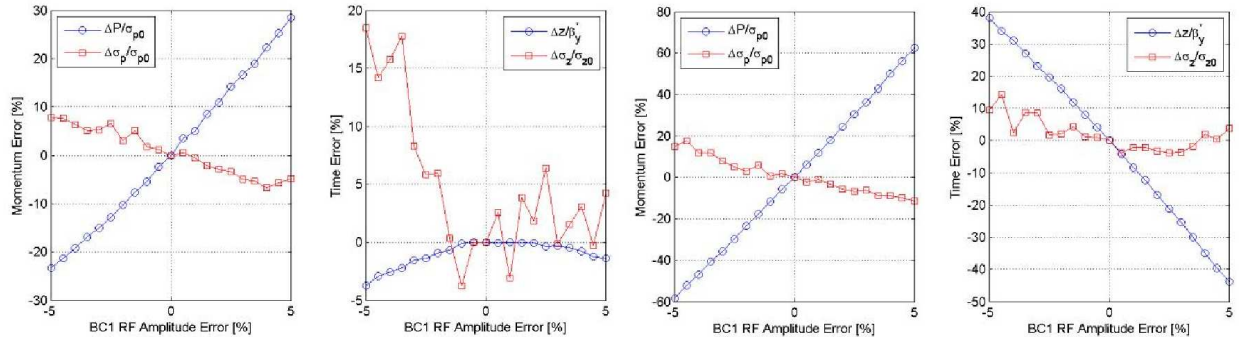

FIG. 24: BC1 RF amplitude error comparison (TAO): G3 150A (left) vs. G3 150B (right)

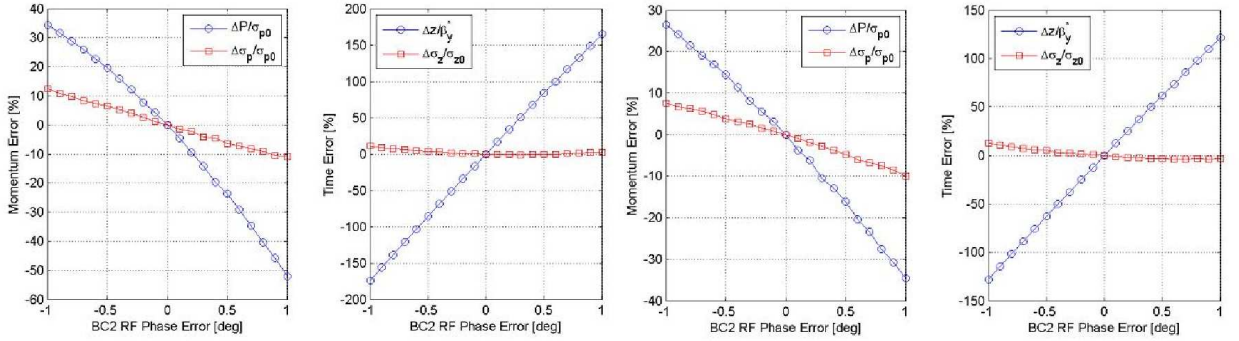

FIG. 25: BC2 RF phase error comparison (Merlin): G1 150A (left) vs. G1 150B (right)

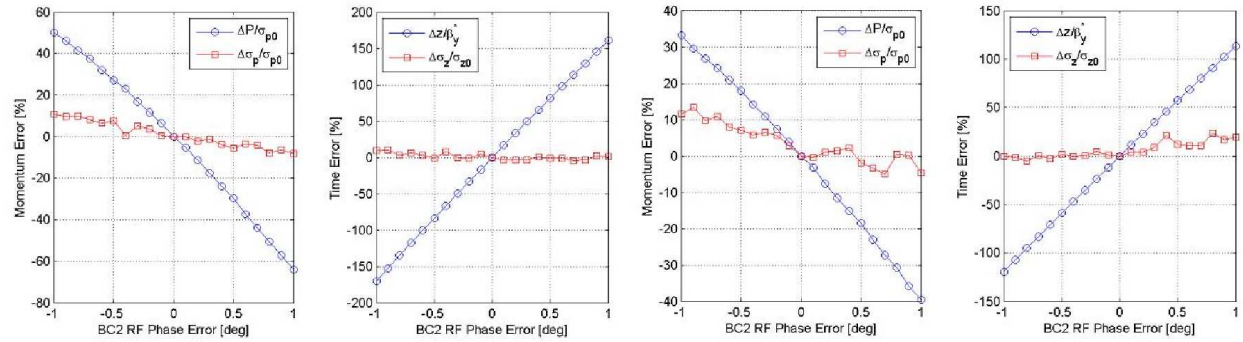

FIG. 26: BC2 RF phase error comparison (TAO): G3 150A (left) vs. G3 150B (right)

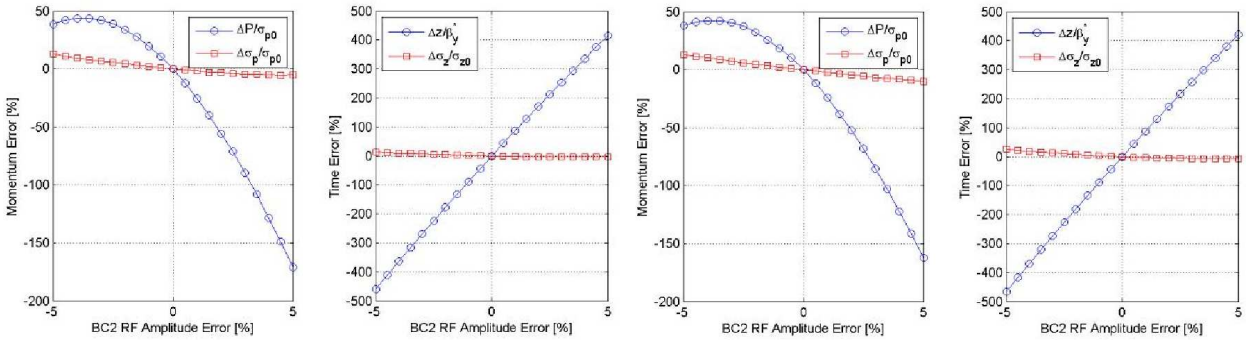

FIG. 27: BC2 RF amplitude error comparison (Merlin): G1 150A (left) vs. G1 150B (right)

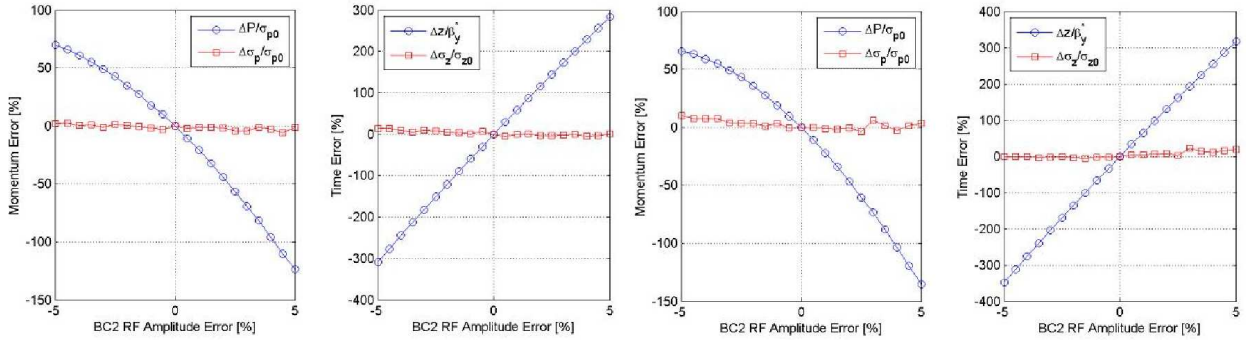

FIG. 28: BC2 RF amplitude error comparison (TAO): G3 150A (left) vs. G3 150B (right)

V. CONCLUSIONS

Various studies have been presented and discussed concerning three potential bunch compressor designs for the International Linear Collider. Each design is able to compress a bunch from 6 mm to 300 μm. The single-stage design produces a higher rms energy spread and more nonlinear distortion to the longitudinal phase space distribution of the bunch than the two-stage designs. Of particular interest, is the comparison of the two different two-stage designs which are able to achieve final rms bunch lengths of 150 μm. Comparisons have been made of the emittance growth and orbit from a 1 σ_y vertical offset, longitudinal tolerances, and emittance growth from synchrotron radiation. The emittance preservation between the two designs are about the same with a one σ_y vertical offset, but with the same offset the G3 150B design achieves a smaller orbit than the G3 150A design. The G3 150B design also has much less emittance growth from incoherent synchrotron radiation than the G3 150A design. Finally, the arrival time sensitivity to various errors for the G3 150B design improves more from the modified G1 design than the G3 150A design does from the its related G1 design.

VI. ACKNOWLEDGMENTS

I would like to thank Prof. Gerald Dugan of Cornell University for his support and for proposing this REU project. I would also like to thank Dr. Andy Wolski of Lawrence Berke-

ley National Laboratory for his knowledge and guidance throughout this project, graduate student Jiajun Xu with whom I worked closely throughout the duration of this research, Jeff Smith and Prof. David Sagan both from Cornell University for their help, and Prof. Lawrence Gibbons, also from Cornell University, among many others who have assisted me in various ways throughout this project. I would also like to acknowledge Prof. Rich Galik for organizing the LEPP Summer REU Program at Cornell University and for all the time and support he has given. This work was supported by the National Science Foundation REU grant PHY-0243687 and research co-opertaive agreement PHY-9809799.

---

[1] T.O. Raubenheimer, "Suggested ILC Beam Parameter Range," (2005).

[2] Andy Wolski, "Relaxing the Bunch Length Specification in ILC Damping Rings," slide 2 (23 March 2005)

[3] For a study of how bunch compression works see "A Short Introduction to Bunch Compressors for Linear Colliders," by Andy Wolski, (8 June 2003) Available at http://www.desy.de/∼njwalker/uspas/

[4] "Tesla TDR Technical Design Report," DESY 2001-011, March 2001

[5] http://www.slac.stanford.edu/∼quarkpt/lucretia

[6] The Tool for Accelerator Optics (TAO) was developed at Cornell University by David Sagan and Jeff Smith. Refer to http://www.lepp.cornell.edu/∼dcs/bmad for more information

[7] Peter Tenenbaum, "LET: Bunch Compressor Design Studies," http://www-project.slac.stanford.edu/ilc/acceldev/LET/BC/G1BC.htm, (8 August 2005)

[8] SLAC results for this Bunch Compressor design can be found at http://www-project.slac.stanford.edu/ilc/acceldev/LET/BC/OneStageBC.html

[9] http://www.desy.de/∼merlin

[10] P. Tenenbaum, T.O. Raubenheimer, and A. Wolsky, "Multi-Stage Bunch Compressors for the International Linear Collider", SLAC-PUB-11214, May 2005. 3pp.

[11] Peter Tenenbaum, "LET: Bunch Compressor Design Studies," http://www-project.slac.stanford.edu/ilc/acceldev/LET/BC/, (8 August 2005)

[12] Private communication with Gerald Dugan (Cornell University) and Andy Wolski (LBNL)

[13] Andy Wolski, "A Short Introduction to Bunch Compressors for Linear Colliders," p. 12, (8 June 2003)

[14] This was calculated via Helms' Method. See "Evaluation of Synchrotron Radiation Integrals" by R.H. Helm, M.J. Lee, and P.L. Morton, SLAC-PUB-1193, A, March 1973

[15] Private communication with Andy Wolski (LBNL)